Milling Experiments on g-TiAl

Milling experiments on γ-TiAl

Priarone P.C., Rizzuti S., Rotella G. and Settineri L.
Politecnico di Torino, Dept. of Production Systems and Business Economics, Turin,
paoloclaudio.priarone@polito.it, stefania.rizzuti@polito.it, giovanna.rotella@polito.it,
luca.settineri@polito.it

Milling experiments on γ-TiAl

Abstract
Advanced structural materials for high temperature applications are often required in aerospace and automotive application. Gamma titanium aluminides (γ-TiAl) show an attractive combination of favourable strength-to-weight ratio, refractoriness, oxidation resistance, high elastic modulus and strength retention at elevated temperatures, together with good creep properties. Unfortunately such properties, along with high hardness and brittleness at room temperature, surface damage, short and unpredictable tool life, undermine their machinability, so that γ-TiAl are regarded as difficult-to-cut materials. A deeper knowledge of their machinability is therefore still required. In this context the paper presents the results of milling experiments conducted on a gamma titanium aluminide of aeronautic interest, aimed at investigating the influence of cutting parameters and cooling conditions on tool wear and surface finish.
Keywords: Milling, Wear, Surface Roughness, γ-TiAl.

1 INTRODUCTION

Gamma titanium aluminides are heat resistant intermetallic alloys, candidates to be used as an alternative to Ni-based superalloys for thermally and mechanically stressed components in aerospace and automotive engines [1-3]. Usually, a γ-TiAl alloy contains 44-48 atomic % Al, with element additions of Cr or Mn to increase ductility, and Nb to improve strength and oxidation resistance. The properties of γ-TiAl consist of low density (approximately half that of Ni superalloys), high stiffness, high refractoriness and high temperature strength. Furthermore, they show fatigue resistance values close to 100% of yield strength [3]. On the other hand, γ-TiAl alloys are less resistant and less flexible if compared with Ni-based superalloys. In spite of their numerous advantages, γ-TiAl alloys show some drawbacks: low ductility at room temperature, which typically ranges between 0.3% and 4% in terms of elongation at rupture (depending on composition and microstructure), together with low fracture toughness. Furthermore, they are considered as difficult-to-cut materials, due to relatively low thermal conductivity, high elevated temperature strength, low ductility, and chemical reactivity with many tool materials [4-7]. In addition, these alloys result to be very sensitive to strain rate, with a strong tendency to hardening. Finally, the saw-tooth chip shape, the built up edge and the presence of abrasives in the alloy microstructure contribute to accelerated wear of the cutting edge, large crater wear on the rake face and chipping phenomena. This fact results in surface hardening, residual stresses, poor finish and the presence of microcracks, impairing fatigue strength of the finished component [7]. Nevertheless, the interest for gamma titanium aluminides applications is high and there still is a need for further studies, particularly to fully understand the machinability of these alloys with conventional or non-conventional processes. In this paper the results of an experimental campaign aimed at

investigating the machinability of a γ-TiAl alloy produced via Electron Beam Melting (hereafter EBM) are reported. Milling experiments have been conducted with varying cutting speed, feed and lubrication conditions. Machining results are analyzed in terms of tool wear and surface conditions.

2 EXPERIMENTAL DETAILS

The milling tests were carried out on a γ-TiAl rectangular-shape specimen, obtained via EBM and subsequently thermally treated. EBM is an additive manufacturing process for metal parts, that starts from powders and melts them layer after layer with an electron beam in a high vacuum. Unlike some metal sintering techniques, the parts are almost fully dense and void-free. The high vacuum makes it suited to manufacture parts in reactive materials with high affinity for oxygen, e.g. titanium [8,9].
The process is followed by a heat treatment to improve density and release residual stresses. The applied heat treatment was 5 hours at 1095 °C, then hot isostatic pressing for 4 hours at 1285 °C, then 2 hours at 1305 °C. The chemical composition of the alloy is listed in Table 1, while the main properties at room temperature are reported in Table 2. Furthermore, the specimen showed an average initial hardness of 273 HV_{30} (with a standard deviation of 5.2 HV_{30}).

Element	**Weight %**
Aluminum	32.0 - 33.5
Niobium	4.5 - 5.1
Chromium	2.2 - 2.6
Oxygen	Max 0.08
Nitrogen	Max 0.02
Carbon	Max 0.015
Iron	Max 0.04
Hydrogen	Max 0.001
All others	Max 0.05
Titanium	Balance (Max 60%)

Table 1. Chemical composition of γ-TiAl alloy.

Tensile strength	345 MPa
Yield strength (0.2% offset)	276 MPa
Elongation, percent in 4D	0.5

Table 2. Mechanical properties of γ-TiAl alloy.

In order to perform microstructural analysis, some specimens were randomly cut from the workpiece; the samples were ground and polished with suspension of colloidal silica (SPM) up to 0.1 μm abrasive particle size, then etched in a Keller solution of 100 ml H_20, 2.5 ml HNO_3, 1.5 ml HCl and 1 ml HF prior to inspection. Microstructural observations on the material reveal a typical lamellar structure, as shown in Figure 1,

with a different orientation of lamellae. The microstructure is not always homogeneous, as shown in Figure 2, where some porosity can be observed. As expected, the EBM fabrication process does not deliver a material with full density: in the present case, density is expected to be around 98%.

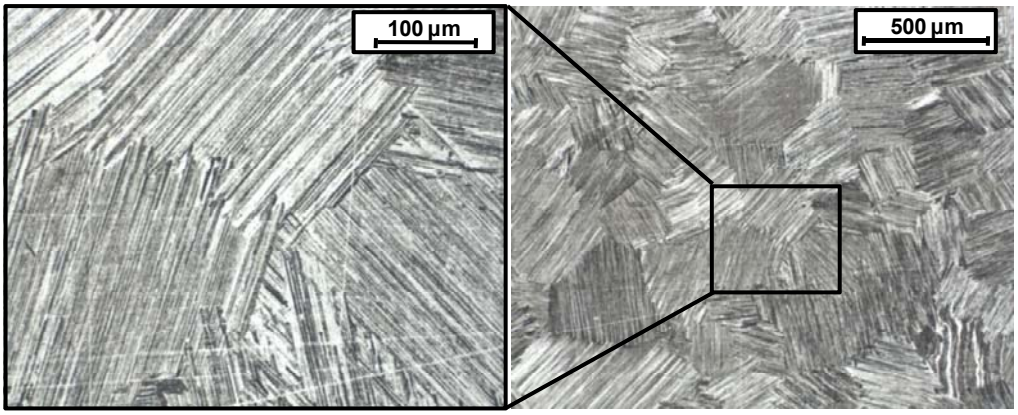

Figure 1. Lamellar microstructure of the sample.

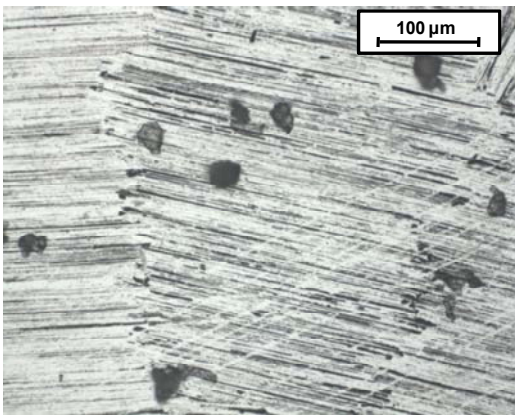

Figure 2. Optical micrograph showing porosity.

The experimental tests were performed using a three axis Cortini M500/F1 vertical CNC milling machine. The machine has a continuously variable spindle that reaches up to 8000 rpm, with a peak power of 3.7 kW and a maximum torque of 24 Nm. Tools used in the experiments were 10 mm diameter Vergnano F405 carbide ISO K30/K40 end mills, with 4 uncoated edges; the cutting tool angle was 12° and the helix angle was 30°. A new cutting tool is illustrated in Figure 3.

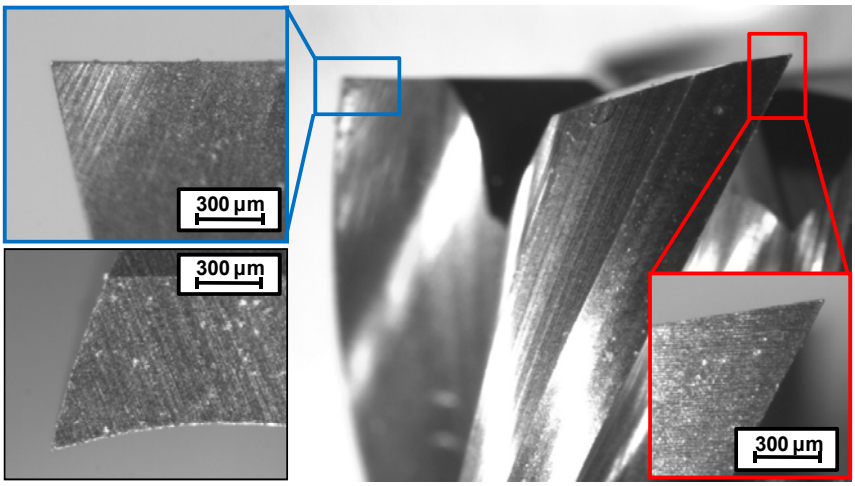

Figure 3. Vergnano F405 new cutting tool.

In order to investigate the alloy's machinability the experimental plan listed in Table 3 was carried out. Axial depth of cut d_a and radial depth of cut d_r have been maintained equal to 0.3 mm, while cutting speed V and feed per tooth f were assumed as independent input variables. More in details, in dry lubrication condition, a full factorial plan 2^2 with a central point was executed. For this point (V = 50 m/min and f = 0.08 mm/tooth) the milling operations were undertaken also in MQL and wet conditions. Finally, being identified the best lubrication condition, comparisons between dry and MQL were analyzed at f = 0.10 mm/tooth and at the varying of the cutting speed V. All the tests were carried out in down-milling direction.

Lubrication	***V*** [m/min]	***f*** [mm/tooth]
DRY	35	0.06
DRY	35	0.10
DRY	50	0.08
DRY	50	0.10
DRY	71	0.06
DRY	71	0.10
WET	50	0.08
MQL	35	0.10
MQL	50	0.08
MQL	50	0.10
MQL	71	0.10

Table 3. Experimental plan.

MQL lubrication was performed by means of a Novatea Accu-Lube Minibooster microlubrication system, with a vegetal lubricant flow of 0.3 ml/min at an air pressure

of 5.5 bar, while wet cutting was carried out with a 5% emulsion of mineral oil in water, with a flow of 10 l/min. Tools were periodically examined in order to measure wear at different cutting times, by means of a stereo microscope Leica MS5 (with 40X magnification), equipped with a high resolution camera Leica DFC280 for image acquisition. The roughness of every milled surface was evaluated by a Hommelwerke Tester T1000 according to EN ISO 4287. The HV_{30} hardness of the generated surface was measured by a Emcotest M4U 025 universal hardness tester, according to the reference standard DIN EN ISO 6507. Microstructural analysis of the material and observation of the generated surface has been performed using an optical microscope Leica MEF4U with magnification up to 1880X, while chip morphology was investigated by a scanning electron microscope LEO 1450 VP, with theoretical resolution equal to 10 nm.

3 RESULTS AND DISCUSSION

3.1 Tool wear and tool life measurement

Tool life measurements were conducted using the above mentioned cutting conditions. The tool wear, which takes into account both the flank and the corner wear (Figure 4), was recorded at regular intervals during machining and for each lubrication condition.

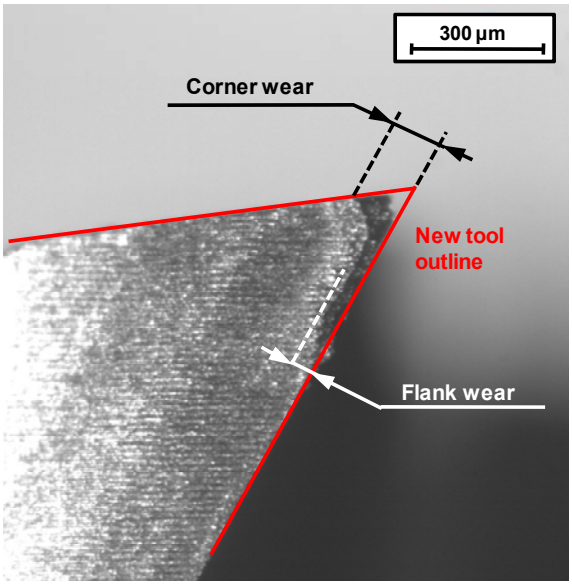

Figure 4. Tool wear measurement criteria.

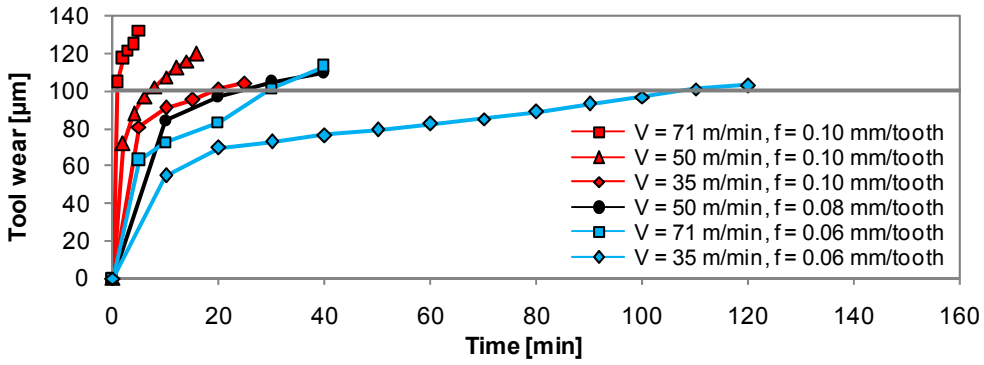

Figure 5. Tool wear curves for dry lubrication condition.

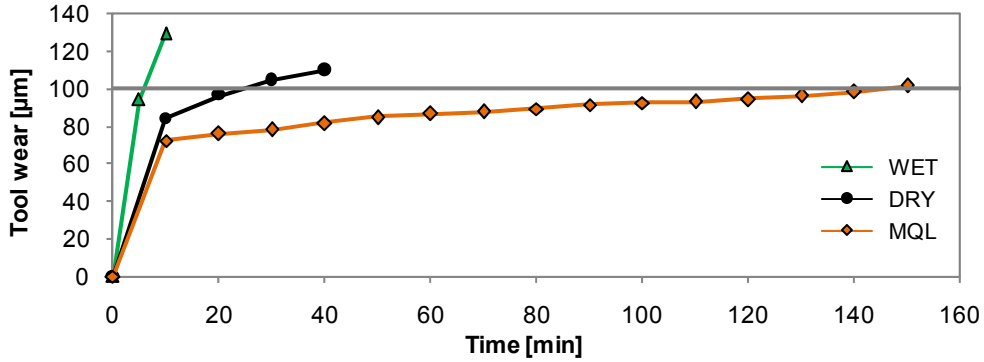

Figure 6. Tool wear curves for the case *V* = 50 m/min and *f* = 0.08 mm/tooth.

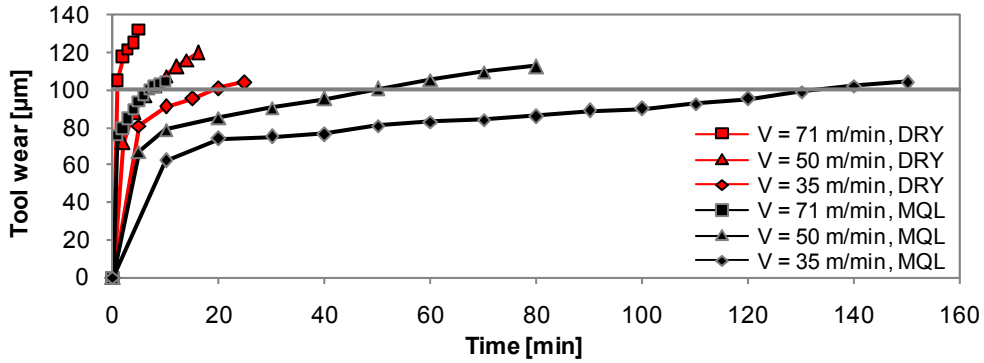

Figure 7. Tool wear curves for the case *f* = 0.10 mm/tooth, comparison between dry and MQL lubrication conditions.

Typical tool wear curves for the tests carried out in dry condition are shown in Figure 5, while in Figure 6 and in Figure 7 the combined effects of lubrication conditions (dry, MQL and wet) and process parameters are evidenced. Each experimental point plotted into the graphs is the average value of the wear measured on the four edges of the mill. The wear limit was fixed to 100 μm. This restrictive condition has been chosen since the surface integrity and finishing of a component made of γ-TiAl alloy is a critical requirement that must meet the severe specifications of the aerospace industry: in fact excessively worn tools generate more deformations, with surface hardening, residuals stresses and poor finish. Tool life estimation results are summarized in Figure 8. In dry lubrication condition tool wear increases by increasing the feed per tooth and the cutting speed. At fixed process parameters (V = 50 m/min and f = 0.08 mm/tooth), Figure 6 highlight that the longer tool life was obtained using MQL cooling condition: in particular, tool life of 5.8 minutes was measured in wet condition, while 24.2 minutes and 145.1 minutes were respectively observed for dry and MQL cooling conditions. In the case of wet cutting, the cutting edge abrupt cooling causes severe thermal shocks, leading to the breakage of the cutting edge. This explains the very low tool life achieved. The tool life of the MQL process, in addition, is bigger than the others in all the investigated cases and, as a general trend, it increases by decreasing the cutting speed.

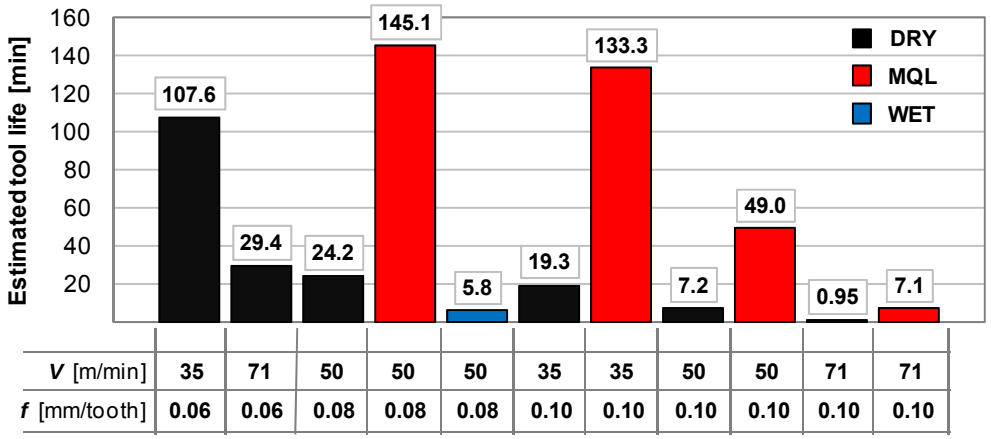

V [m/min]	**35**	**71**	**50**	**50**	**50**	**35**	**35**	**50**	**50**	**71**	**71**
f [mm/tooth]	**0.06**	**0.06**	**0.08**	**0.08**	**0.08**	**0.10**	**0.10**	**0.10**	**0.10**	**0.10**	**0.10**

Figure 8. Tool life estimation.

3.2 Surface hardness

Figure 9 reports some results in terms of machined surface hardness versus cutting time. Each point in the graph represents the average value of five experimental measurements. The effects of processing time are evident: hardness increases as a result of strain hardening due to tool wear, and this phenomenon is common to all tests performed. As for the effects of the cutting parameters, in dry lubrication

condition it can be assessed that the surface hardness increases as the feed per tooth increases. On the other hand the dependence on the cutting speed is more complex: Figure 9a shows that, for the case of f = 0.06 mm/tooth, with fresh tools, hardness is lower at higher cutting speed. This is due to the softening induced by the higher temperature generated by the higher speed. With worn tools, strain hardening due to tool wear prevails.

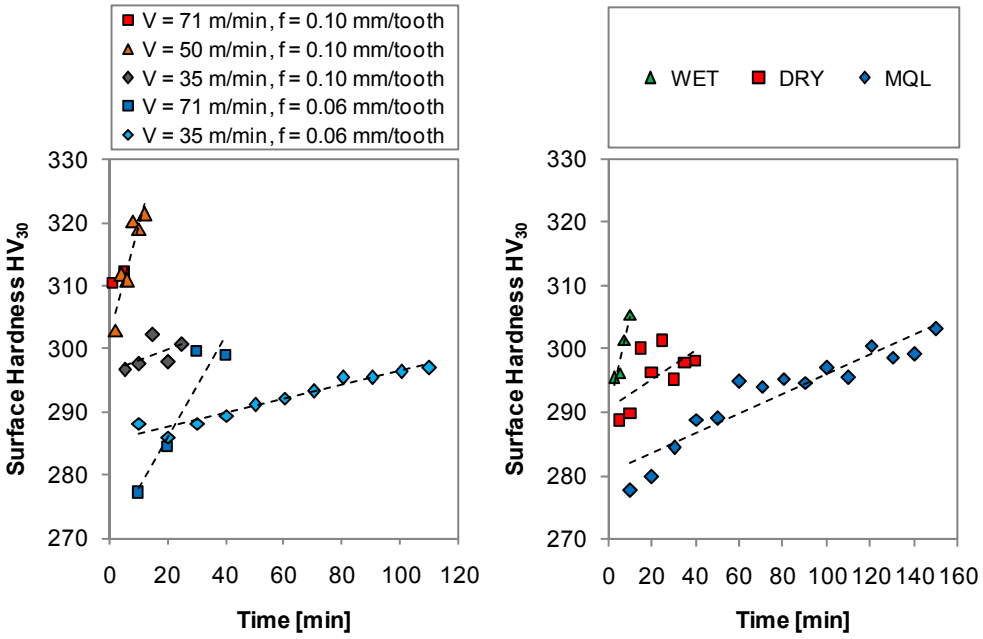

(a) (b)

Figure 9. Hardness of the generated surface, for dry lubrication condition (a) and for the case V = 50 m/min and f = 0.08 mm/tooth (b).

3.3 Surface Roughness

The roughness of the machined sample was measured in order to evaluate the characteristic of the surface. In particular, mean average, Ra, the average maximum height of the profile, Rt, the skewness, Rsk, and the curtosis roughness, Rku, were measured. It is important to remember that Rsk and Rku are important roughness indexes when the machined surface bearing capabilities needs to be investigated, especially for aerospace applications. The results, as shown in Table 4, demonstrate that each process presents acceptable profiles as far as the surface quality is concerned. In particular, the maximum height of the profile ranged between 1.54 and 3.03 μm while the Ra value varied from 0.19 to 0.32 μm. The skewness resulted to be less than 0 in all the considered tests while Rku was almost always more than 3.

Lubrication	***V*** [m/min]	***f*** [mm/tooth]	**Ra** [µm]	**Rt** [µm]	**Rsk**	**Rku**
DRY	35	0.06	0.22	1.73	-0.03	3.17
DRY	35	0.10	0.31	2.62	-0.05	3.28
DRY	50	0.08	0.22	1.81	-0.12	3.31
DRY	50	0.10	0.24	2.03	-0.09	3.25
DRY	71	0.06	0.19	1.54	-0.07	3.25
DRY	71	0.10	0.22	1.66	-0.05	2.98
WET	50	0.08	0.26	2.38	-0.36	3.44
MQL	35	0.10	0.28	2.46	-0.20	3.35
MQL	50	0.08	0.28	2.52	-0.28	3.45
MQL	50	0.10	0.27	2.46	-0.19	3.38
MQL	71	0.10	0.32	3.03	-0.26	3.53

Table 4. Measured roughness.

In dry conditions Ra and Rt present a clear trend versus the cutting speed and the feed per tooth. As expected, Ra and Rt decrease as the cutting speed increases and the feed per tooth decreases. On the other hand, Rku and Rsk show a more complex dependence at the increasing of both the cutting speed and feed per tooth: Rku shows a maximum for the intermediate cutting speed and feed, and decreases thereafter; Rsk behaves exactly in the opposite way. This effect may be due to the characteristics of the observed chip formation mechanism. For intermediate values of cutting speed and feed, strain hardening of the chip material generates micro craters on the machined surface, being this fact reinforced by the not perfectly homogeneous microstructure of a material obtained via a powder melting process [10,11]. As the cutting speed and feed increase, the heat generated by the higher strain rate, makes the chip material flow smoother and less prone to generate chipping on the generated surface. The effects of lubrication conditions on the surface roughness do not follow strictly the indications of the literature, being the results for dry cutting slightly better than in the other cases [7 and ref. therein]. This is confirmed by the micro-photographies of the surface shown in Figure 10. The higher friction coefficient of the dry cutting generates higher temperatures and a more regular chip detachment mechanism, with a smoother generated surface.

3.4 Chip morphology

The chips were collected and analyzed for each performed test. Figure 11 shows, with different magnifications, the chip morphology observed by SEM for the case f = 0.06 mm/tooth and V = 71 m/min, for dry lubrication condition. For all the cutting and lubrication conditions the chip appears discontinuous and with a saw tooth shape. The saw tooth pitch depends on cutting speed and feed, as expected.

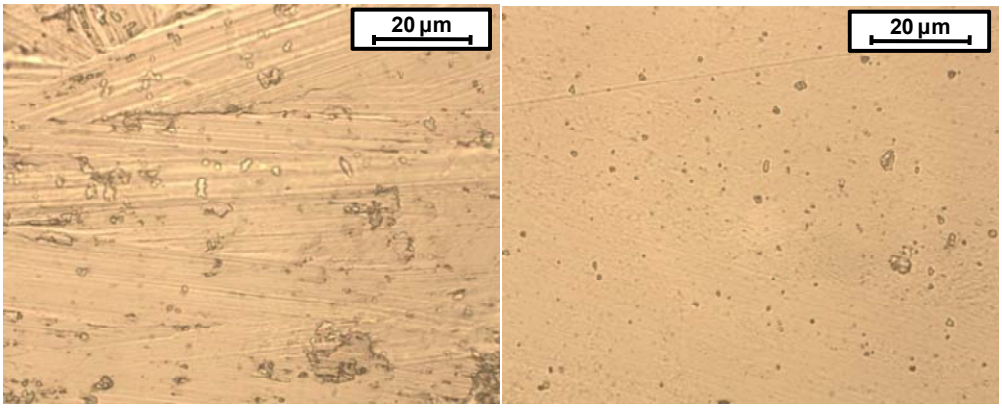

(a) (b)

Figure 10. Micrograph of the generated surface (1000X), for V = 50 m/min and f = 0,08 mm/tooth, MQL (a) and dry (b) lubrication conditions.

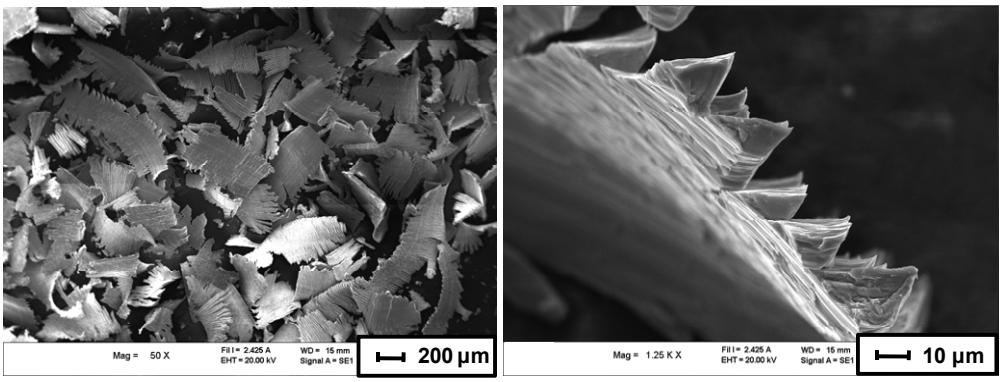

(a) (b)

Figure 11. Chip morphology for V = 71 m/min and f = 0,06 mm/tooth, magnification 50X (a) and 1250X (b).

4 CONCLUSIONS

In this paper, the results of milling experiments conducted on a particular γ-TiAl alloy for aerospace applications, fabricated via Electron Beam Melting, are presented. Machining tests have been performed with different cutting speeds, feeds, and lubrication conditions. Tool wear and surface finish were evaluated for each case. The tests show that tool wear increases by increasing the feed per tooth and the cutting speed. Analysis of the results under different lubrication conditions shows that MQL is

by far the method that allows the highest tool life. Surface roughness and hardness also show dependence on the cutting parameters, at least in the explored range. The observed chips evidenced a sawtooth shape for all the tests. Further investigations will be focused on process analysis, in order to evaluate the effects of tool geometry (cutting angles and cutting edge pre-treatment) as well as of advanced tool coatings on tool wear and surface integrity.

REFERENCES

[1] Weinert, K., Bergmann, S., Kempmann, C., 2006. Machining sequence to manufacture a γ-TiAl-conrod for application in combustion engines, *Adv. Eng. Mater*., 8, pp. 41-47.

[2] Austin, C. M., 1999. Current status of gamma titanium aluminides for aerospace applications, *Current opinion in solid state and materials science*, 4, pp. 239-242.

[3] Loria, E. A., 2000. Gamma titanium aluminides as a prospective structural materials, *Intermetallics*, 8, pp.1339-1345.

[4] Mantle, A. L., Aspinwall, D. K., 2006. Cutting force evaluation when high speed end milling a gamma titanium aluminide intermetallic alloy, in *Intermetallics and Superalloys*, 10, *Editors: D. G. Morris, S. Naka, P. Caron, Wiley On line library.*

[5] Aspinwall, D. K., Dewes, R. C., Mantle, A. R., 2005. The machining of γ-TiAl intermetallic alloys, *Annals of the CIRP*, 54/1, pp. 99-104.

[6] Mantle, A. R., Aspinwall, D. K., 2001. Surface integrity of a high speed milled gamma titanium aluminide, *Journal of Materials Processing Technology*, 118, pp. 143-150.

[7] Sharman, A. R. C., Aspinwall, D. K., Dewes, R. C., Bowen, P., 2001. Workpiece surface integrity considerations when finish turning gamma titanium aluminide, *Wear*, 249, pp. 473-481.

[8] Cormier, D., Harrysson, O., Mahale, T., West, H., 2007. Freeform fabrication of titanium aluminide via electron beam melting using prealloyed and blended powders, *Research Letters in Materials Science, Hindawi Publishing Corporation*, pp.1-4.

[9] Yu, K. O., 2001. Modeling for casting & solidification processing, *Series Materials Engineering, Taylor & Francis Group.*

[10] Petropoulos, G. P., Pandazaras, C. N., Davim, J. C., West, H., 2010. Surface texture characterization and evaluation related to machining, in *Surface Integrity in Machining, Springer-Verlag, London Limited, UK.*

[11] Cotterell, M., Byrne, G., 2008. Dynamics of chip formation during orthogonal cutting of titanium alloy Ti-6Al-4V, *Annals of the CIRP*, 57/1, pp. 93-96.